Organic Electronics 23 (2015) 208–212

Contents lists available at ScienceDirect

Organic Electronics

journal homepage: www.elsevier.com/locate/orgel

Highly efficient and color stable single-emitting-layer fluorescent WOLEDs with delayed fluorescent host

Bo Zhao [a,b], Tianyou Zhang [a,b], Wenlian Li [a,*], Zisheng Su [a,*], Bei Chu [a], Xingwu Yan [a,b], Fangming Jin [a,b], Yuan Gao [a,b], Hairuo Wu [a,b]

[a] State Key Laboratory of Luminescence and Applications, Changchun Institute of Optics, Fine Mechanics, and Physics, Chinese Academy of Sciences, Changchun 130033, People's Republic of China
[b] University of Chinese Academy of Sciences, Beijing 100039, People's Republic of China

ARTICLE INFO

Article history:
Received 13 March 2015
Received in revised form 4 May 2015
Accepted 5 May 2015
Available online 5 May 2015

Keywords:
WOLED
Single-emitting-layer
Delayed fluorescence
TADF

ABSTRACT

We demonstrated highly efficient and color stable single-emitting-layer fluorescent WOLEDs using blue thermally activated delayed fluorescent material of bis[4-(9,9-dimethyl-9,10-dihydroacridine)phenyl]sulfone (DMAC-DPS) as host and traditional orange fluorescent material of (5,6,11,12)-tetraphenyl-naphthacene (rubrene) as dopant. At a low dopant concentration of 0.6 wt%, we achieved the efficient white emission that comprised of blue host and orange dopant. The maximum current efficiency, power efficiency and external quantum efficiency were 20.2 cd A^{-1}, 15.9 lm W^{-1} and 7.48%, respectively. Besides, the Commission Internationale de l'Eclairage coordinates were almost the same with the increased voltage, which shifted from (0.359, 0.439) to (0.358, 0.430) as the voltage rose from 5 V to 8 V. The achievement of so high efficiency was attributed to the efficient up-conversion of DMAC-DPS triplet excitons and efficient energy transfer from host to dopant by Förster transfer mechanism. The more detailed working mechanism was also argued.

1. Introduction

In recent years, the appearance of thermally activated delayed fluorescent (TADF) materials open up a new research field involved with organic light emitting diodes (OLEDs) [1–3]. An important feature of this kind of material is the small singlet–triplet energy splitting (ΔE_{S-T}) [4–6], which employs the triplet excitons could up-convert to the singlet excited state (S_1) via efficient reverse intersystem crossing (RISC). Finally, 100% singlet excitons could be harvested by radiative transition theoretically. Adachi and coworkers have pioneered various highly efficient TADF materials with the emission of blue, green and red [7–9].

On the other hand, except for as the fluorescent emitter, the TADF material has another new application, that is, as the host of electroluminescence (EL) devices thanks to their intrinsic small ΔE_{S-T}. In generally, it is well recognized that under electrically excitation, the ratio of singlet and triplet excitons formed on host is 1:3 [10,11]. In theory, the TADF host could transfer 100% singlet excitons to dopant owing to the existence of efficient RISC process. Nakanotani et al. reported fluorescence-based OLEDs that realized external quantum efficiencies as high as 13.4–18% for blue, green, yellow and red emission by utilizing TADF molecules as assistant dopants to form the cascade energy transfer scheme [12]. Qiu group demonstrated high-efficiency yellow fluorescent OLEDs with the external quantum efficiency (EQE) of 12.2% using TADF materials of 2,4-diphe-nyl-6-bis(12-phenylindolo)[2,3-a]carbazole-11-yl-1,3,5-triazine (DIC-TRZ) as the sensitizing host [13]. These reports were exciting and realized the highly efficient fluorescent OLED with traditional fluorescent emitters.

In terms of above mentioned progress, we expect to design white OLEDs (WOLEDs) with a simple single-emitting-layer structure in which blue TADF material and traditional orange fluorescent material as the host and dopant, respectively. WOLEDs that derived from both the emissions of host and dopant would be demonstrated through an incomplete energy transfer from the blue TADF host to orange fluorescent dopant. The similar single-emitting-layer structures WOLEDs had been developed many years, and the emitting layer (EML) was composed of blue fluorescent host and orange fluorescent dopant or blue fluorescent host and orange phosphorescent dopant commonly [14–18]. Phosphor doped WOLEDs could achieve 100% internal quantum efficiency (IQE) due to the separated transfer channel of singlet and triplet excitons [14,15]. But the devices suffered from the high

* Corresponding authors.
E-mail addresses: wllioel@aliyun.com (W. Li), suzs@ciomp.ac.cn (Z. Su).

http://dx.doi.org/10.1016/j.orgel.2015.05.009
1566-1199/

cost with heavy metal of Iridium and instable white spectra with increased voltages [15,16]. Fluorophor doped WOLEDs had the advantage of low cost and high stability, but the limit of 5% EQE could not satisfy the requirement of practical application [17,18]. But the TADF host made it possible for highly efficient fluorophor doped WOLEDs. The 75% triplet excitons produced on TADF host could up-convert to its S_1, then the total singlet excitons of >25% would transfer to S_1 of dopant by Förster energy transfer process. Besides, the Dexter energy transfer between triplet excited state (T_1) of host and dopant could be suppressed effectively by decreasing the doped concentration [19]. Because the >25% singlet excitons are harvested through efficient RISC, the WOLEDs of >5% EQE would be achieved expectedly.

In this paper, we chose bis[4-(9,9-dimethyl-9,10-dihydroacridine)phenyl]sulfone (DMAC-DPS) as blue TADF host and (5,6,11,12)-tetraphenyl-naphthacene (rubrene) as orange fluorescent dopant, respectively. DMAC-DPS is an highly efficient blue TADF material with small ΔE_{S-T} of 0.08 eV in m-bis(N-carbazolyl)benzene (mCP) film [9]. Rubrene is a very traditional orange fluorescent material. By the optimal dopant concentration, we achieved highly efficient white emission with the current efficiency, power efficiency and EQE of 20.2 cd A^{-1}, 15.9 lm W^{-1} and 7.48%, respectively; meanwhile, the WOLEDs exhibited stable EL spectra and the Commission Internationale de l'Eclairage (CIE) coordinates changed only from (0.359, 0.439) to (0.358, 0.430) when the voltages increased from 5 V to 8 V. The high EQE of above 5% indicates efficient RISC of DMAC-DPS host and efficient Förster energy transfer from DMAC-DPS to rubrene, which is confirmed from the transient photoluminescence (PL) decay measurement.

2. Experiments methods

Indium tin oxide (ITO) coated glass substrates were cleaned routinely and treated with ultraviolet-ozone for 15 min before loading into a high vacuum deposition chamber ($\sim 3 \times 10^{-4}$ Pa). The organic materials were purchased commercially without further purification. Absorption spectrum was measured with UV–VIS-NIR scanning spectrophotometer (Shimadzu, UV-3101PC). Steady-state PL and EL spectra were measured with F7000 and OPT-2000 spectrophotometer, respectively. Transient PL decay was measured with a combination of Nd-YAG laser (pulse width of 10 ns, repetition frequency of 10 Hz), spectrograph (HJY, Triax 550) and oscilloscope (Tektronix, TDS3052B). The electrical characteristics of the WOLEDs were measured with a Keithley model 2400 power supply combined with a ST-900 M spot photometer and were recorded simultaneously with measurements. EQE was calculated from the current density, luminance and spectra data. All measurements were carried out at room temperature and under ambient conditions without any protective coatings.

3. Results and discussion

Fig. 1 shows the PL spectrum of DMAC-DPS and absorption spectrum of rubrene. We see that the PL peak of DMAC-DPS lies at 470 nm, as reported in Ref. [9]. The large spectral overlap between host PL spectrum and dopant absorption spectrum indicates the energy transfer from S_1 of DMAC-DPS to S_1 of rubrene by Förster mechanism could take place efficiently. The device structures of our single-emitting-layer fluorescent WOLEDs are ITO/MoO_3 (3 nm)/TCTA (20 nm)/host: 0.6 wt% rubrene (15 nm)/Bphen (40 nm)/LiF (1 nm)/Al, where the host are DMAC-DPS and 4,4′-bis(9-ethyl-3-carbazo-vinylene)-1,1′-biphenyl (BCzVBi), and the corresponding devices are referred as Device A and Device B, respectively. Here, hole transport layer (HTL) and electron transport layer (ETL) are TCTA (4,4′,4″-tri(N-carbazolyl)triphenylamine) and Bphen (4,7-diphenyl-1,10-phenanthroline),

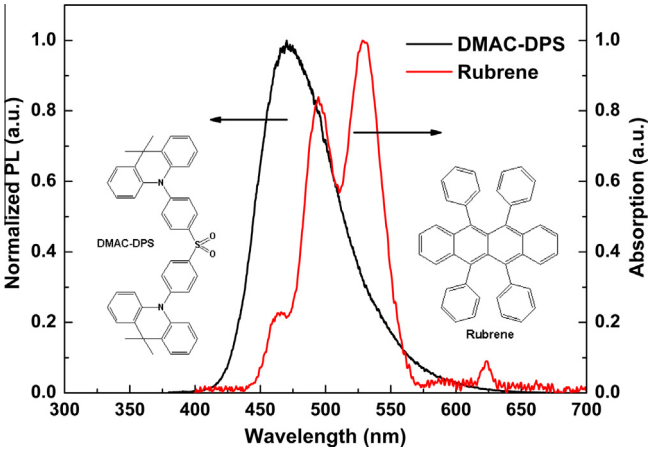

Fig. 1. The PL spectrum of DMAC-DPS and absorption spectrum of rubrene.

respectively. As a reference, we chose BCzVBi as the common blue fluorescent host.

Fig. 2 shows the energy level diagram and electrical characteristics of the optimized WOLEDs with current density, luminance, current efficiency, power efficiency and EQE curves. From Fig. 2(a), we can see that Device A exhibits a lower turn-on voltage of 2.48 V than Device B with 2.98 V. This could be understood by the almost zero of carrier injection barrier from the electron and hole transport layers to EML. Fig. 2(b) shows the energy level diagram of the WOLEDs. The lowest unoccupied molecular orbital (LUMO) and highest occupied molecular orbital (HOMO) levels of DMAC-DPS are 2.92 eV and 5.92 eV, respectively [9]. The LUMO of ETL (Bphen) is 3.0 eV, only 0.08 eV electron injection barrier presents at EML/ETL interface. Similarly, the HOMO of TCTA that acts as HTL is 5.90 eV, a lower hole injection barrier of 0.02 eV exists at HTL/EML interface. Besides, the separated donor and acceptor units on DMAC-DPS molecule would balance the transport of electron and hole in EML. Therefore, Device A shows the extremely low turn-on voltage. Fig. 2(c) and (d) plot the current efficiency, power efficiency and EQE curves. The maximum current efficiency, power efficiency and EQE of Device A are 20.2 cd A^{-1}, 15.9 lm W^{-1} and 7.48%, respectively. Even at the luminance of 1000 cd m^{-2}, the efficiencies can still remain at 19.8 cd A^{-1}, 14.7 lm W^{-1} and 7.31%, respectively. While Device B with traditional blue fluorescent material of BCzVBi as the host only obtain a relative low maximum current efficiency, power efficiency and EQE of 11.1 cd A^{-1}, 6.9 lm W^{-1} and 3.72%, respectively. Table 1 summarizes the data of the two WOLEDs in this paper.

The achievement of so high EQE for Device A indicates that the triplet excitons produced on DMAC-DPS host could up-convert to its S_1 easily due to the presence of small ΔE_{S-T}, and then the singlet excitons are transferred partly to rubrene by Förster transfer mechanism. While for Device B, because a large ΔE_{S-T} of BCzVBi molecule (>0.2 eV) [20] and a low dopant concentration of 0.6 wt%, the up-conversion of triplet excitons from T_1 to S_1 and Dexter energy transfer from BCzVBi to rubrene would not be so efficient so that the triplet excitons on BCzVBi would be only non-radiative transition to ground state, which lead to the low EL efficiency. In terms of above performance comparison between Device A and B, the most perfect energy transfer and EL emission processes in this system are described schematically, as shown in Fig. 3. The Dexter energy transfer between T_1 of host and dopant could be minimized by an extremely low dopant concentration (0.6 wt%). In terms of theory, we could achieve 20% EQE supposing the 100% IQE and 20% coupled out efficiency. But in fact, we only earn the EQE of 7.48%, which is far away from the theoretical upper limit. One hand, we consider the increase of non-radiative decay

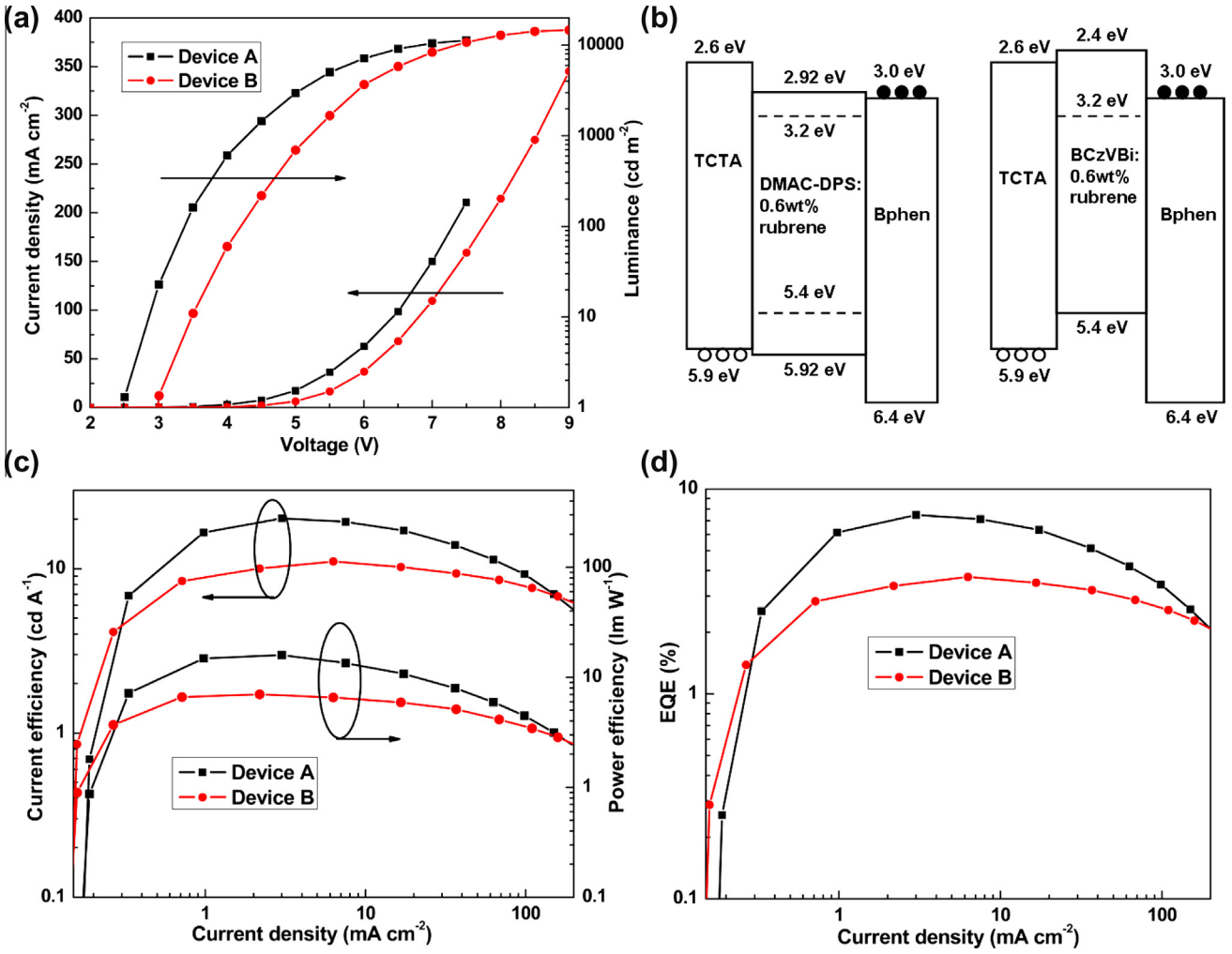

Fig. 2. The energy level diagram and electrical characteristics of the optimized WOLEDs. (a) Current density–voltage–Luminance, (b) the energy level diagram, (c) current efficiency–current density–power efficiency and (d) EQE–current density.

Table 1
The summary on EL data of Device A and Device B in this paper.

	V_{on}[a] [V]	$\eta_{c,Max.}/\eta_{p,Max.}/EQE_{Max}$[b] [cd A^{-1}/lm W^{-1}/%]	$\eta_{c,1000}/\eta_{p1000}/EQE_{1000}$[c] [cd A^{-1}/lm W^{-1}/%]	$\eta_{c,10,000}/\eta_{p10,000}/EQE_{10,000}$[d] [cd A^{-1}/lm W^{-1}/%]
Device A	2.48	20.2/15.9/7.48	19.8/14.7/7.31	7.8/3.6/2.90
Device B	2.98	11.1/6.9/3.72	10.8/6.3/3.64	7.1/3.0/2.37

[a] Turn-on voltage.
[b] Current efficiency (η_c), power efficiency (η_p) and EQE at maximum.
[c] η_c, η_p and EQE at 1000 cd m^{-2}.
[d] η_c, η_p and EQE at 10000 cd m^{-2}.

rate due to the high host concentration reduces the RISC efficiency; on the other hand, the Dexter energy transfer between T_1 of host and dopant must occurs partly, which is disadvantageous and should be prevented in this system. In addition, the LUMO of rubrene is close to the LUMO of DMAC-DPS, so the trap of electron could be suppressed efficiently. But the HOMO of rubrene is far away from the HOMO of DMAC-DPS and the hole could be trapped by rubrene molecule. Therefore, the trap process cannot be avoided completely in this system, which also influences the EL performance of WOLEDs [21].

Fig. 4 exhibits the EL spectra of Device A and Device B. It is well known that the spectral stability of WOLEDs is very significance for the application either displays or solid state lighting. To our great

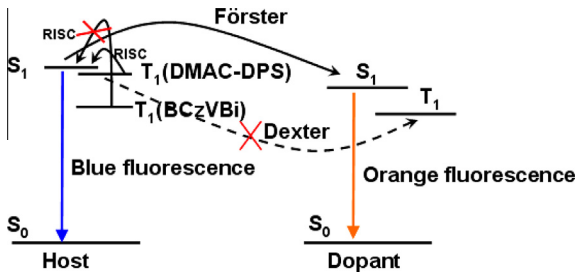

Fig. 3. The most perfect energy transfer and EL emission processes in this system.

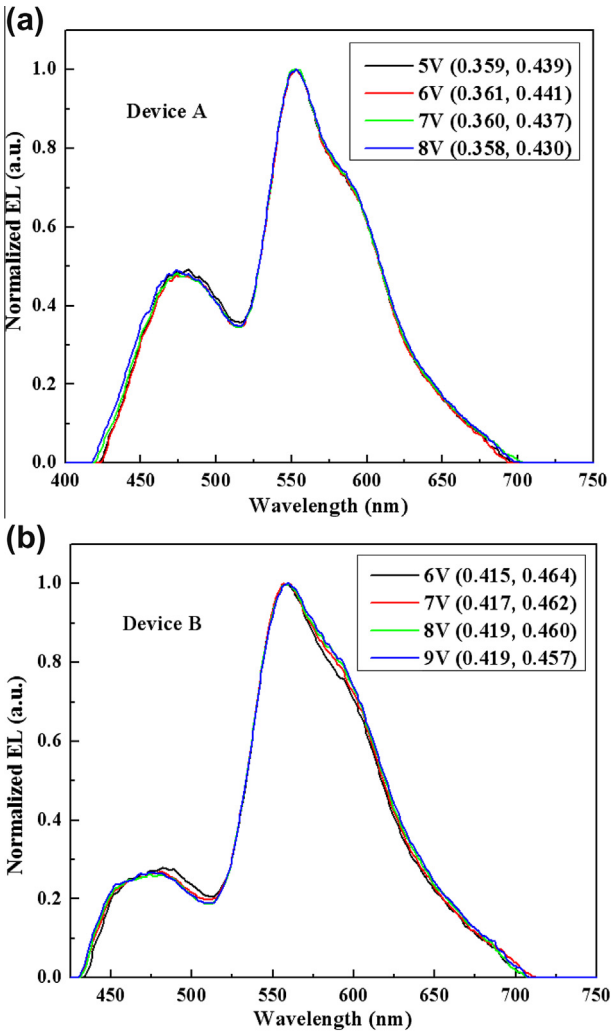

Fig. 4. The EL spectra of Device A and Device B.

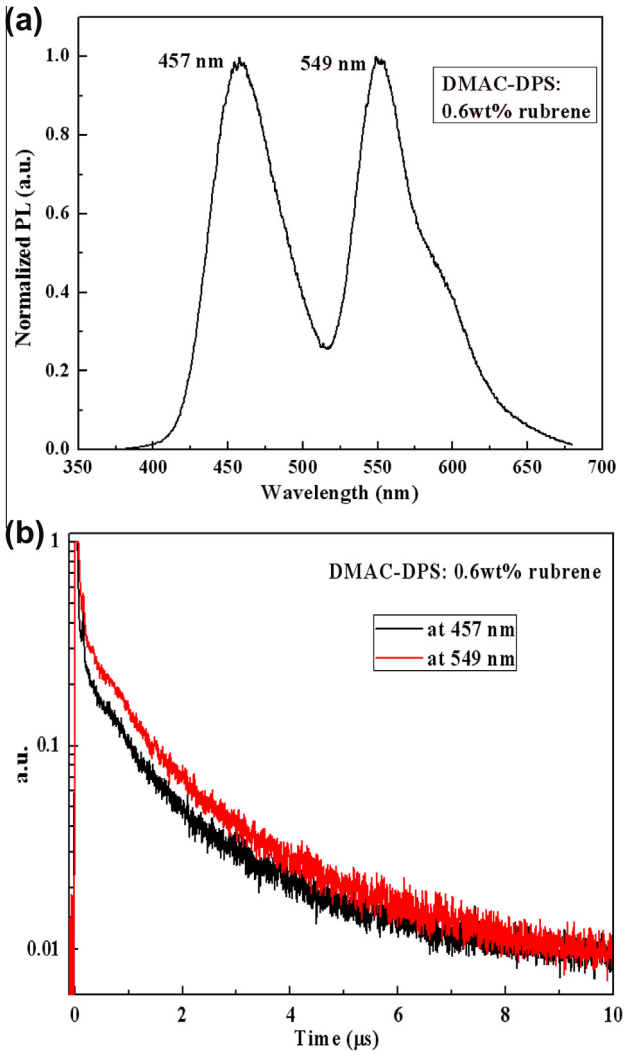

Fig. 5. The PL spectrum and transient PL decay curve of the film of DMAC-DPS: 0.6 wt% rubrene.

surprise, Device A with DMAC-DPS as the host shows excellent spectral stability and the emissive sub-bands of host blue and guest orange could also be recognized clearly. Meanwhile, Device A get a stronger emission of blue and better CIE coordinates compared to Device B. The white EL spectra of Device A are less changed with increased voltages. The CIE coordinates of Device A shift from (0.359, 0.439) to (0.358, 0.430) as the voltage rises from 5 V to 8 V. The excellent spectral stability with increased voltages could be ascribed to balanced injection, transport and recombination of electron and hole [22]. The interface barriers at HTL/EML and EML/ETL are almost zero in Device A, which resulted in the balanced injection of carriers. Besides, the design of donor–acceptor units in DMAC-DPS molecule balanced the transport of carriers in EML. The balanced injection and transport lead to the balanced recombination of electrons and holes. Therefore, the WOLEDs offer a desirable spectral stability, which is in favor of displays and solid sate lighting applications.

In order to further understand the energy transfer process in Device A, the transient PL decay characteristics were measured. Fig. 5 plots the PL spectrum and transient PL decay curve of 0.6 wt% rubrene doped into DMAC-DPS film. We can see that the PL spectrum of the mixed film comprises two emission peaks, 457 nm and 549 nm, which are assigned to the emissions from DMAC-DPS host and rubrene dopant, respectively. Fig. 5(b) depicts the transient PL decay curves of doped film mentioned above under different emission peaks. DMAC-DPS is a TADF material with charge transfer feature, which has two excited state lifetimes of prompt and delayed components [9]. In our case, monitoring the emission peaks of DMAC-DPS, a prompt component of 43 ns and a delayed component of 1.04 μs are also observed clearly. But the delayed component we measured is shorter compared to that reported in Ref. [9] (3.1 μs), which may be result from the increase of concentration quenching. Besides, rubrene is a general fluorescent material with a very short lifetime of several nanoseconds, but we also observed a similar two lifetime components comprises of 61.6 ns and 1.17 μs from the emission of rubrene in the film of DMAC-DPS: 0.6% rubrene, respectively. Based on the two PL components from the emission of rubrene, we could confirm that the emission of rubrene stems from an efficient energy transfer from DMAC-DPS host, including the energy transfer of delayed component. We also carried out the transient PL decay of mixed film of BCzVBi: 0.6 wt% rubrene, but there is only one prompt component under the two emission peaks. Such a result would further prove that the efficient RISC processes exist in Device A and the energy transfer from DMAC-DPS to rubrene under electrically excitation is also proved by the transient PL decay measurement.

4. Conclusions

In conclusion, we fabricated single-emitting-layer fluorescent WOLEDs utilizing TADF material of DMAC-DPS as blue fluorescent

host and traditional material of rubrene as orange fluorescent dopant. Through the incomplete energy transfer from DMAC-DPS to rubrene, the simple WOLEDs achieved the emissions of host and dopant simultaneously and exhibited high current efficiency, power efficiency and EQE with 20.2 cd A^{-1}, 15.9 lm W^{-1} and 7.48%, respectively. Meanwhile, the WOLEDs exhibited stable EL spectra and the CIE coordinates changed only from (0.359, 0.439) to (0.358, 0.430) when the voltage increased from 5 V to 8 V. The achievement of so high efficiency was attributed to efficient up-conversion of triplet excitons and efficient Förster energy transfer from DMAC-DPS to rubrene, which were proved from the transient PL decay measurement. Our design provides a very promising technology for developing WOLEDs and higher efficiency could be demonstrated as long as more efficient blue TADF materials are selected or synthesized and better device structures are designed.

Acknowledgment

This work was supported by the National Natural Science Foundation of China (61376022, 61376062, 61107082 and 11004187).

References

[1] A. Endo, M. Ogasawara, A. Takahashi, D. Yokoyama, Y. Kato, C. Adachi, Adv. Mater. 21 (2009) 4802.
[2] A. Endo, K. Sato, K. Yoshimura, T. Kai, A. Kawada, H. Miyazaki, C. Adachi, Appl. Phys. Lett. 98 (2011) 083302.
[3] G. Mehes, H. Nomura, Q. Zhang, T. Nakagawa, C. Adachi, Angew. Chem. Int. Ed. 51 (2012) 11311–11315.
[4] T. Nakagawa, S.Y. Ku, K.T. Wong, C. Adachi, Chem. Commun. 48 (2012) 9580–9582.
[5] Q. Zhang, J. Li, K. Shizu, S. Huang, S. Hirata, H. Miyazaki, C. Adachi, J. Am. Chem. Soc. 134 (2012) 14706–14709.
[6] K. Sato, K. Shizu, K. Yoshimura, A. Kawada, H. Miyazaki, C. Adachi, Phys. Rev. Lett. 110 (2013) 247401.
[7] H. Uoyama, K. Goushi, K. Shizu, H. Nomura, C. Adachi, Nature 492 (2012) 234.
[8] S. Hirata, Y. Sakai, K. Masui, H. Tanaka, S.Y. Lee, H. Nomura, N. Nakamura, M. Yasumatsu, H. Nakanotani, Q. Zhang, K. Shizu, H. Miyazaki, C. Adachi, Nat. Mater. 14 (2015) 330.
[9] Q. Zhang, B. Li, S. Huang, H. Nomura, H. Tanaka, C. Adachi, Nat. Photonics 8 (2014) 326–332.
[10] T. Tsutsui, S. Saito, Nato Asi Series, vol. 246, Kluwer Academic publisher, 1993, pp. 123–134.
[11] L.J. Rothberg, A.J. Lovinger, J. Mater. Res. 11 (1996) 3174–3187.
[12] H. Nakanotani, T. Higuchi, T. Furukawa, K. Masui, K. Morimoto, M. Numata, H. Tanaka, Y. Sagara, T. Yasuda, C. Adachi, Nat. Commun. 5 (2014) 4016.
[13] D. Zhang, L. Duan, C. Li, Y. Li, H. Li, D. Zhang, Y. Qiu, Adv. Mater. 26 (2014) 5050–5055.
[14] X.K. Liu, C.J. Zheng, M.F. Lo, J. Xiao, Z. Chen, C.L. Liu, C.S. Lee, M.K. Fung, X.H. Zhang, Chem. Mater. 25 (2013) 4454–4459.
[15] J. Ye, Z. Chen, F. An, M. Sun, H.W. Mo, X. Zhang, C.S. Lee, ACS Appl. Mater. Interfaces 6 (2014) 8964–8970.
[16] J. Ye, K. Wang, Z. Chen, F.F. An, Y. Yuan, C. Zhang, X.H. Zhang, C.S. Lee, Org. Electron. 15 (2014) 3514–3520.
[17] G. Li, J. Shinar, Appl. Phys. Lett. 83 (2003) 5359.
[18] L. Duan, D. Zhang, K. Wu, X. Huang, L. Wang, Y. Qiu, Adv. Funct. Mater. 21 (2011) 3540–3545.
[19] Y. Zhang, M. Slootsky, S.R. Forrest, Appl. Phys. Lett. 99 (2011) 223303.
[20] G. Schwartz, S. Reineke, T.C. Rosenow, K. Walzer, K. Leo, Adv. Funct. Mater. 19 (2009) 1319–1333.
[21] X.-K. Liu, Z. Chen, C.-J. Zheng, M. Chen, W. Liu, X.-H. Zhang, C.-S. Lee, Adv. Mater. 27 (2015) 2025–2030.
[22] Y.S. Park, J.W. Kang, D.M. Kang, J.W. Park, Y.H. Kim, S.K. Kwon, J.J. Kim, Adv. Mater. 20 (2008) 1957–1961.